Host–Guest Chemistry

International Edition: DOI: 10.1002/anie.201812926
German Edition: DOI: 10.1002/ange.201812926

Chiral Self-Discrimination and Guest Recognition in Helicene-Based Coordination Cages

*Thorben R. Schulte, Julian J. Holstein, and Guido H. Clever**

Abstract: *Chiral nanosized confinements play a major role for enantioselective recognition and reaction control in biological systems. Supramolecular self-assembly gives access to artificial mimics with tunable sizes and properties. Herein, a new family of $[Pd_2L_4]$ coordination cages based on a chiral [6]helicene backbone is introduced. A racemic mixture of the bis-monodentate pyridyl ligand $\mathbf{L^1}$ selectively assembles with Pd^{II} cations under chiral self-discrimination to an achiral meso cage, cis-$[Pd_2\mathbf{L^{1P}}_2\mathbf{L^{1M}}_2]$. Enantiopure $\mathbf{L^1}$ forms homochiral cages $[Pd_2\mathbf{L^{1P/M}}_4]$. A longer derivative $\mathbf{L^2}$ forms chiral cages $[Pd_2\mathbf{L^{2P/M}}_4]$ with larger cavities, which bind optical isomers of chiral guests with different affinities. Owing to its distinct chiroptical properties, this cage can distinguish non-chiral guests of different lengths, as they were found to squeeze or elongate the cavity under modulation of the helical pitch of the helicenes. The CD spectroscopic results were supported by ion mobility mass spectrometry.*

Nanosized cages based on metallosupramolecular self-assembly have become major players in host–guest chemistry owing to their structural and functional variability and modular composition.[1] Recent design-based approaches allow the positioning of multiple building blocks by thermodynamically controlled integrative self-sorting.[2] In biological host–guest systems, enantioselective recognition plays a pivotal role because of the inherent homochirality of most natural compounds. Hence, the formation of synthetic chiral hosts for enantioselective guest binding is not only of fundamental interest, but provides the basis for the development of selective sensors, transporters, and catalysts.[3]

Numerous chiral hosts based on covalent macrocyclic molecules such as cyclodextrins, cyclophanes, and calixarenes have been reported.[4] Chirality has also been reported to facilitate the assembly of hydrogen-bonded organic cages.[5] More recently, chiral metallo-supramolecular self-assembled rings and cages have been introduced as selective receptors and enzyme-like nanoreactors based on chiral backbones, auxiliaries, the inherent chirality of stereogenic metal centers, or the overall architecture.[6] Upon metal coordination, racemic mixtures of ligands may undergo chiral self-sorting,[7] leading to homochiral[8–10] or heterochiral[10,11] assemblies. Beyond their use in enantioselective recognition, chiral cages based on luminescent metal centers have been shown to exhibit unique chiroptical properties.[9,12] With respect to mechanically interlocked coordination cages,[13] reports covering the implementation of homochirality are still scarce, with Hardie's dimer of cyclotriveratrylene-based coordination cages serving as a notable example.[14]

Since their discovery in 1912,[15] helicenes have been widely studied for properties related to their helical chirality.[16] While helicenes have shown appearance in several supramolecular systems, they have never been used in the construction of coordination-driven cages.[17] We herein demonstrate that despite their highly twisted appearance, helicene-based bis-monodentate ligands can be used to assemble discrete $[Pd_2\mathbf{L}_4]$ coordination cages exhibiting chirality-driven effects on their assembly and guest binding. We further report the first example of a homochiral interpenetrated $[Pd_4\mathbf{L}_8]$ dimer, comprising eight interlocked helicenes.

Ligands $\mathbf{L^1}$ and $\mathbf{L^2}$ were synthesized by Sonogashira cross-coupling reactions from literature-known 2,15-dibromo-[6]helicene (Figure 1) to yield racemic products, which were separated into the enantiomers by chiral HPLC (see the Supporting Information, Figure S23).[18] Following our previously reported routines, the bis-monodentate ligands were tested for the formation of self-assembled products using $[Pd(CH_3CN)_4](BF_4)_2$ as the metal source in different polar organic solvents. Interestingly, in deuterated dimethyl sulfoxide (DMSO), the racemic mixture of ligand $\mathbf{L^1}$ was found to quantitatively assemble under chiral self-sorting into the achiral *meso* cage *cis*-$[Pd_2\mathbf{L^{1P}}_2\mathbf{L^{1M}}_2]$ ($\mathbf{C1^{meso}}$), containing both ligand enantiomers in a 1:1 ratio, as confirmed by ^{1}H (Figure 2a) and NOESY NMR spectroscopy (Figure 4b). For all herein described cages, the ^{1}H NMR signals of the pyridine moieties (i.e., protons H_a and H_b) undergo a downfield shift upon coordination to the palladium(II) cations. The formation of the *meso* cage leads to splitting of all ^{1}H NMR resonances into two sets of equal intensity. All resonances could be assigned with the help of 2D NMR techniques (COSY, NOESY, HSQC), indicating that the upper and lower halves of ligand $\mathbf{L^1}$ have ended up in a different surrounding upon cage formation (see the Supporting Information). The resonance splitting can be explained by symmetry considerations. The halves of the *P* helicenes and the halves of the *M* helicenes facing each other have the same chemical surrounding, which results in the same chemical shifts for

[*] Dr. T. R. Schulte, Dr. J. J. Holstein, Prof. Dr. G. H. Clever
Faculty of Chemistry and Chemical Biology
TU Dortmund University
Otto-Hahn-Str. 6, 44227 Dortmund (Germany)
E-mail: guido.clever@tu-dortmund.de
Supporting information and the ORCID identification number(s) for the author(s) of this article can be found under: https://doi.org/10.1002/anie.201812926.

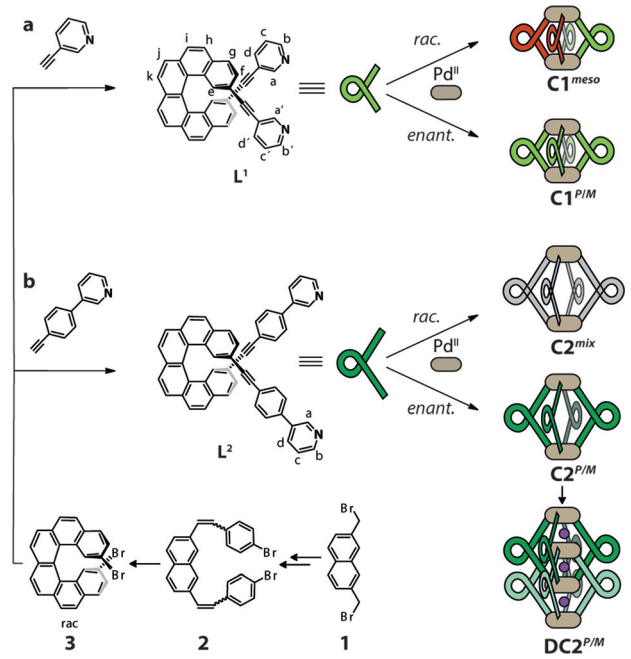

Figure 1. a, b) Synthesis of ligands $\mathbf{L^1}$ and $\mathbf{L^2}$ from 2,15-dibromo-[6]helicene **3** followed by separation into the *P* (red) and *M* (green) enantiomers. The addition of stoichiometric amounts of Pd^{II} leads to the quantitative formation of different coordination cages, depending on the enantiomeric composition and length of the ligand. Racemic $\mathbf{L^1}$ exclusively gives $\mathbf{C1^{meso}}$, whereas racemic $\mathbf{L^2}$ leads to a statistical mixture of all possible stereoisomers (*PPPM*/*MMMP*/*PPMM*/*PMPM*/*PPPP*/*MMMM*, shown in gray). The enantiopure ligands give the chiral coordination cages $\mathbf{C1^{P/M}}$ and $\mathbf{C2^{P/M}}$ and the interpenetrated dimer $\mathbf{DC2^{P/M}}$.

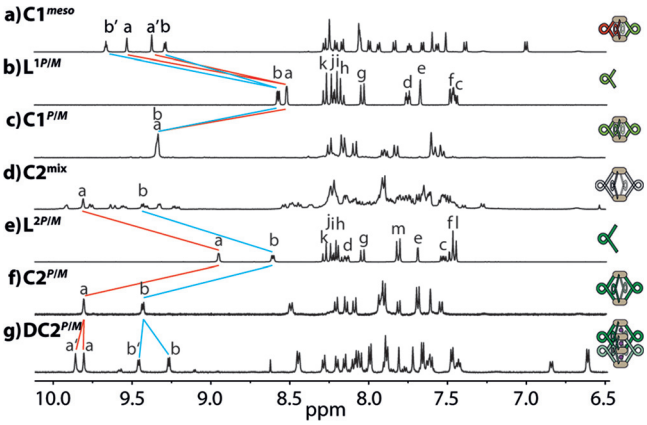

Figure 2. ^{1}H NMR spectra (400 MHz, [D$_6$]DMSO, 293 K) of: a) $\mathbf{C1^{meso}}$, b) $\mathbf{L^{1P/M}}$, c) homochiral $\mathbf{C1^{P/M}}$, d) a statistical mixture of **C2** stereoisomers, e) $\mathbf{L^{2P/M}}$, f) homochiral $\mathbf{C2^{P/M}}$, and g) the homochiral interpenetrated cage structure $\mathbf{DC2^{P/M}}$ (here: 600 MHz, [D$_3$]acetonitrile, 293 K).

the corresponding protons. Compared to this, one half of the *P* helicene facing the other half of the *P* helicene (same for *M* helicenes) has a different chemical surrounding, which explains the twofold splitting in the ^{1}H NMR spectrum. A tentative *trans*-configured cage would not lead to such a splitting of the NMR signals as the resulting D_{2d} symmetry would offer two C_2 axes perpendicular to the major C_2 axis going through both Pd centers, which would allow converting the upper half of each ligand into its lower part (Figure S7).

In contrast, assembly with the enantiopure ligand $\mathbf{L^1}$, in either its *P* or *M* form, leads to a homochiral cage with no splitting of the ^{1}H NMR signals (Figure 2c). In their high-resolution ESI mass spectra, cage $\mathbf{C1^{meso}}$ (Figure S9) and the enantiopure cages $\mathbf{C1^{P/M}}$ (Figure S11) could be identified as tetracationic $[Pd_2\mathbf{L^1}_4]^{4+}$.

Next, chiral guest discrimination of $\mathbf{C1^P}$ was tested with (1*R*)- and (1*S*)-camphorsulfonate anions ($\mathbf{G1^R}$ and $\mathbf{G1^S}$); however, no evidence for uptake of the guests was found (Figure S21). The most probable reason is the limited size of the cavity, known as a critical factor for guest binding.[19] To permit guest encapsulation, the ligand structure was extended by including 1,4-phenylene linkers on both sides to give ligand $\mathbf{L^2}$. The elongation of the ligands nearly doubles the Pd–Pd distance in the modeled structures (DFT ωB97XD/def2SVP, PCM solvent: DMSO) of $\mathbf{C2^{P/M}}$ (20.1 Å; Figure 4d) compared to $\mathbf{C1^{P/M}}$ (10.4 Å; Figure 4c). In case of racemic $\mathbf{L^2}$, cage formation leads to the splitting of all ^{1}H NMR resonances into several sets, which is indicative of a lack of chiral self-sorting under formation of a statistical mixture of isomeric species (Figure 2d). This picture is supported by the clean appearance of the high-resolution ESI mass spectrum of this mixture, showing only peaks assignable to the tetracationic $[Pd_2\mathbf{L^2}_4]^{4+}$ species, which is superimposable with the spectrum of the homochiral cage $\mathbf{C2^{P/M}}$ (Figure S14). The absence of chiral self-discrimination upon cage formation from racemic $\mathbf{L^2}$ can be explained with the increased distance between the helicene backbones (based on the calculated structures of cages **C1** and **C2**, the closest H–H distance between two neighboring backbones has increased from 2.39 Å to 6.20 Å).

In contrast to the results obtained in DMSO, heating the enantiopure ligand $\mathbf{L^2}$ with palladium(II) cations in acetonitrile was found to lead to a splitting of all NMR resonances into two sets of equal intensity, thus indicating the formation of a chiral interpenetrated cage $\mathbf{DC2^{P/M}}$ (Figure 2g).[13] In addition, the high-resolution ESI mass spectrum contained signals for the dimeric species $[3BF_4@Pd_4\mathbf{L^2}_8]^{5+}$ (Figure 3c).

Further structural insight was obtained by X-ray diffraction methods. Crystals of enantiopure $\mathbf{L^2}$ (second HPLC fraction eluted from a Chiralpak IC column) suitable for X-ray structure analysis were obtained by crystallization from DMSO (Figure 4e). The asymmetric unit contains twelve individual helicene ligands, all of which are highly intertwined in a remarkably unordered fashion (Figure S25). The absolute configuration was unambiguously determined as the *P* enantiomer using the method of Parsons[20] as implemented in SHELXL,[21] yielding an enantiopurity-distinguishing parameter of $x = 0.079(8)$. This assignment is in agreement with the recorded circular dichroism (CD) spectra of this compound as compared to published data on similarly substituted [6]helicenes and DFT-calculated CD bands.[22,23]

Single crystals of the dimeric cage species $[2\,PF_6@Pd_4\mathbf{L^{2M}}_8]$ ($\mathbf{DC2^M}$, based on the *M* ligand enantiomer eluting first from the chiral column) that were suitable for X-ray structure analysis were obtained by slow diffusion of diethyl ether into an acetonitrile solution of the cage containing PF_6^- counter-

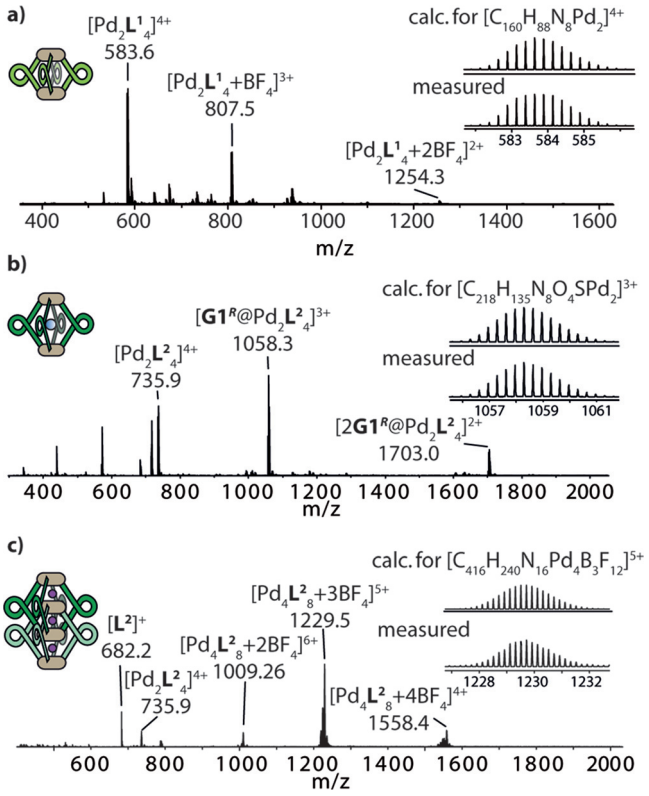

Figure 3. ESI mass spectra of: a) cage **C1**^{M}, b) cage **C2**^{M} after addition of (1*R*)-camphorsulfonate **G1**^{R}, and c) double cage **DC2**^{M}.

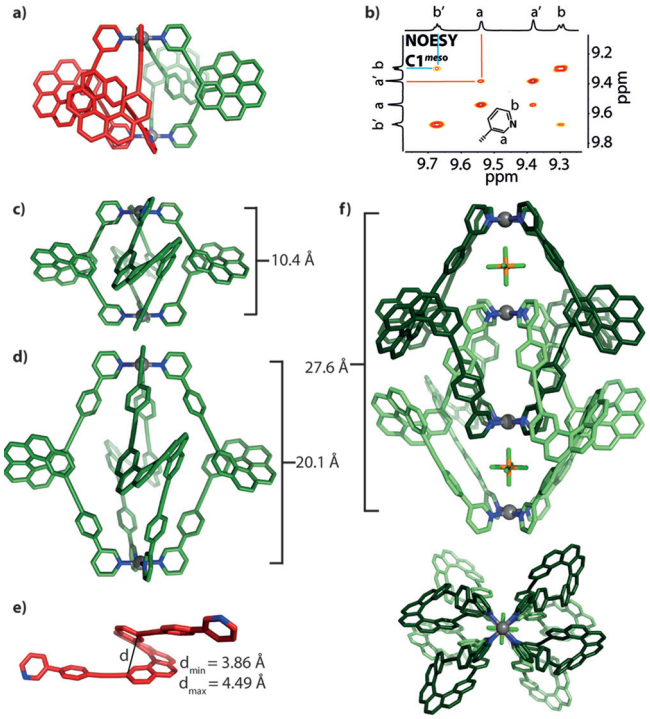

Figure 4. a) DFT-calculated structure of **C1**^{meso}. b) NOESY NMR detail of the **C1**^{meso} cage supporting the *cis* ligand arrangement. c, d) Calculated structures of **C1**^{M} and **C2**^{M}. e) One of twelve **L**^{2P} molecules in the asymmetric unit of its solid-state structure with the found minimum/maximum helical pitches. f) X-ray crystal structure of **DC2**^{M}, side and top view along the Pd_4 axis. Pd gray, N blue, C green (*M* enantiomer) and red (*P* enantiomer), P orange, F light green).

anions (Figure 4 f). Synchrotron radiation was required to obtain diffraction data that could be solved with direct methods using SHELXT.[24] Again, the absolute configuration could be unambiguously determined, yielding an enantiopurity-distinguishing parameter of $x = -0.02(2)$. The CD data were found to be in agreement with the literature-reported absolute structure assignment of comparable helicenes.[22,23] The structure reveals that the double cage features three consecutive pockets, with the two outer ones filled with a PF_6^- anion each. The Pd–Pd distances are 8.66 Å for the outer pockets and 10.33 Å for the inner cavity.

With the large cavity of monomeric **C2**$^{P/M}$, chiral guest discrimination could be shown for the enantiopure cages by ^{1}H NMR titration experiments by stepwise addition of camphorsulfonates **G1**^{R} and **G1**^{S} as their tetrabutylammonium salts. Characteristic downfield shifts for the inside-pointing proton resonance H_a were observed (Figure S22), and the results were summarized as a comparison of binding isotherms ($\Delta\delta$ plot; Figure 5 c). Pleasingly, both guest enantiomers showed different binding behavior when exposed to the same chiral cage; however, the combination **G1**^{S}**@C2**^{P} showed the same behavior as the enantiomeric system **G1**^{R}**@C2**^{M}, with binding constants of around 560 M^{-1}.[25] The diastereomeric combinations to this, **G1**^{R}**@C2**^{P} and **G1**^{S}**@C2**^{M}, showed a stronger extent of NMR signal shifting and a binding constant of approximately 1010 M^{-1}. In the high-resolution ESI mass spectra, the host–guest complexes could be identified as the triple cationic species $[\mathbf{G1}@Pd_2\mathbf{L}^{2}_{4}]^{3+}$ (Figure 3 b).

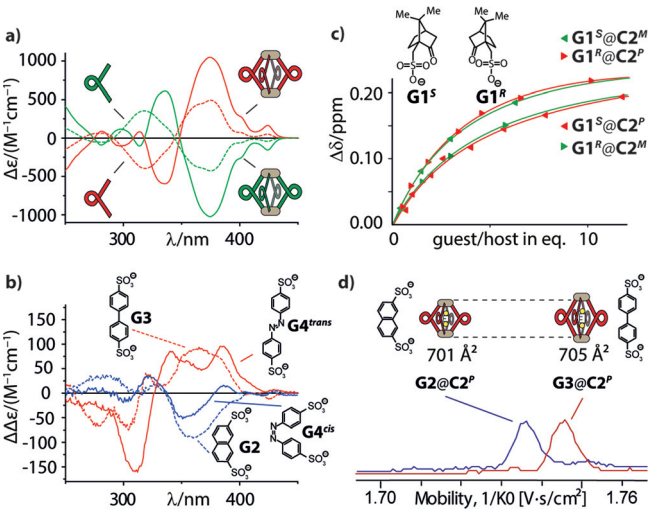

Figure 5. a) Circular dichroism spectra of ligands **L**$^{2P/M}$ and cages **C2**$^{P/M}$. b) Difference CD spectra (free host CD spectra subtracted from the host–guest CD spectra) of **G2@C2**^{P} and **G3@C2**^{P} as well as **G4**^{trans}**@C2**^{P} and **G4**^{cis}**@C2**^{P} (all in DMSO). c) Comparison of the binding isotherms for all four diastereomeric host–guest combinations **G1**$^{R/S}$**@C2**$^{P/M}$ showing two "matched" and two "mismatched" cases. d) Superposition of the mobilograms obtained by trapped ion mobility ESI-TOF mass spectrometry for host–guest complexes **G2@C2**^{P} (mobility $1/K_0$: 1.736 Vs cm^{-2}, CCS: 701 Å^2 at *m/z* 1615.4) and **G3@C2**^{P} (mobility $1/K_0$: 1.745 Vs cm^{-2}, CCS: 705 Å^2 at *m/z* 1627.9).

Furthermore, CD spectra were compared for $\mathbf{L}^{1P/M}$ and $\mathbf{C1}^{P/M}$ (Figure S24) and $\mathbf{L}^{2P/M}$ and $\mathbf{C2}^{P/M}$ (Figure 5a), showing strong circular dichroism for the ligands and the cages with a positive Cotton effect for the *P* enantiomers. We next set out to investigate the potential utilization of the strong CD effect as an indicator for the discrimination of achiral guests. As the cages consist of four helicenes arranged like parallel springs around two connecting Pd^{II} cations, we envisioned that charged guests encapsulated between these electrostatic anchors should modulate the helical pitch of the ligand backbones. First, we compared the effect of binding short 2,7-naphthalenedisulfonate **G2** and long 4,4′-biphenyldisulfonate **G3** on the CD spectra of $\mathbf{C2}^{P}$. Difference spectra revealed that encapsulation of the shorter guest led to a decrease in the intensity of the CD band at approximately 360 nm while binding of the longer guest increased the intensity of the same band (Figure 5b). The assumption that such an effect is caused by tuning of the helical pitch of the helicenes was predicted by theoretical work of Mori, Inoue, and Nakai.[22] We were able to confirm this hypothesis by calculating the relative CD signal intensities of unsubstituted [6]helicene under variation of its helical pitch within the limits found in the twelve individual ligands contained in the solid-state structure of $\mathbf{L}^{2}$ (Figure S26 and Figure 4e).

Furthermore, direct evidence for a shrinking and expansion of the cages upon addition of the short and long guests, respectively, came from trapped ion mobility ESI-TOF mass spectrometry (timsTOF), which indicated a smaller gas phase collisional cross-section for $\mathbf{G2@C2}^{P}$ (701 Å^2) than for $\mathbf{G3@C2}^{P}$ (705 Å^2), even in a mixture of both host–guest complexes (Figure 5d and Figure S27).[26] We repeated the CD experiment with azobenzene-based guest **G4**,[27] either in its *cis* or *trans* photoisomeric form (Figure 5b). Remarkably, the effect of the band intensity decrease/increase could be reproduced and allows differentiation between the *cis* and the *trans* form of achiral azobenzene by CD spectroscopy, keeping in mind that the free guest itself shows no CD effect. In addition, the observed deviations from the expected band shapes were attributed to a certain degree of chirality transfer on the azobenzene chromophore, which—in contrast to guests **G2** and **G3**—shows significant absorption around 360 nm.

In summary, a family of $[Pd_2\mathbf{L}_4]$ coordination cages based on a chiral helicene backbone have been developed.[28] One of the cages showed integrative chiral self-sorting, thus serving as an example of the non-statistical formation of heteroleptic structures, while another one was found to discriminate chiral guests through different binding affinities to its enantiopure form. The strong circular dichroism of the helicene backbone could further be exploited for the size discrimination of achiral anionic guests by taking advantage of modulations of the chiroptical properties of the system upon guest-induced changes of the helical pitch. Ion mobility mass spectrometry was employed to support these findings. In addition, the group of $[Pd_4L_8]$ interpenetrated cages could be expanded by an unprecedented chiral species, as illustrated by its single-crystal X-ray structure. Further studies are underway to expand the guest binding and recognition features and develop a system for enantioselective catalysis inside confined environments.

Experimental Section

Cages **C1** and **C2** were formed by addition of $[Pd(CH_3CN)_4](BF_4)_2$ (0.5 equiv) to the corresponding ligands (racemic or enantiopure) in DMSO at 23 °C. Cage **DC2** was formed after heating **C2** in MeCN at 75 °C for 2 weeks. Single crystals suitable for X-ray structure determination were grown for $\mathbf{L}^{2P}$ from DMSO and for $\mathbf{DC2}^{M}$ by slow diffusion of Et_2O into a mixture of $\mathbf{L}^{2M}$ and $[Pd(CH_3CN)_4](PF_6)_2$ in MeCN at 7 °C. CCDC 1558206 ($\mathbf{L}^{2P}$) and 1581540 ($\mathbf{DC2}^{M}$) contain the supplementary crystallographic data for this paper. These data can be obtained free of charge from The Cambridge Crystallographic Data Centre.

Acknowledgements

This work has been supported by the Deutsche Forschungsgemeinschaft (CL 489/2-2, RESOLV Cluster of Excellence EXC-2033, project number 390677874) and the European Research Council through ERC Consolidator grant 683083 (RAMSES). We thank Prof. U. Diederichsen, Prof. L. Ackermann and Prof. L. Tietze (all Georg-August University Göttingen) for access to CD and HPLC facilities. We further thank S. Löffler for support with crystallization experiments, Prof. W. Hiller (TU Dortmund), Dr. M. John (GAU Göttingen) for help with NMR spectroscopy and L. Schneider (TU Dortmund), C. Heitbrink, Dr. P. Janning (MPI Dortmund), and Dr. H. Frauendorf (GAU Göttingen) for ESI mass spectra. Diffraction data for $\mathbf{DC2}^{M}$ were collected at PETRA III, DESY, a member of the Helmholtz Association (HGF). We thank Saravanan Panneerselvam for assistance in using synchrotron beamline P11 (I-20160736).[29]

Conflict of interest

The authors declare no conflict of interest.

Keywords: anion recognition · chirality · host–guest chemistry · interpenetration · supramolecular chemistry

How to cite: *Angew. Chem. Int. Ed.* **2019**, *58*, 5562–5566
Angew. Chem. **2019**, *131*, 5618–5622

[1] a) R. Chakrabarty, P. S. Mukherjee, P. J. Stang, *Chem. Rev.* **2011**, *111*, 6810; b) M. Han, D. M. Engelhard, G. H. Clever, *Chem. Soc. Rev.* **2014**, *43*, 1848.

[2] a) S. Mukherjee, P. S. Mukherjee, *Chem. Commun.* **2014**, *50*, 2239; b) W. M. Bloch, G. H. Clever, *Chem. Commun.* **2017**, *53*, 8506.

[3] a) A. M. Castilla, W. J. Ramsay, J. R. Nitschke, *Acc. Chem. Res.* **2014**, *47*, 2063; b) L.-J. Chen, H.-B. Yang, M. Shionoya, *Chem. Soc. Rev.* **2017**, *46*, 2555; c) M. Pan, K. Wu, J.-H. Zhang, C.-Y. Su, *Coord. Chem. Rev.* **2019**, *378*, 333.

[4] a) Y. Tsunoda, K. Fukuta, T. Imamura, R. Sekiya, T. Furuyama, N. Kobayashi, T. Haino, *Angew. Chem. Int. Ed.* **2014**, *53*, 7243; *Angew. Chem.* **2014**, *126*, 7371; b) C. Gropp, N. Trapp, F. Diederich, *Angew. Chem. Int. Ed.* **2016**, *55*, 14444; *Angew. Chem.* **2016**, *128*, 14659.

[5] D. Beaudoin, F. Rominger, M. Mastalerz, *Angew. Chem. Int. Ed.* **2016**, *55*, 15599; *Angew. Chem.* **2016**, *128*, 15828.
[6] a) C. J. Carrano, K. N. Raymond, *J. Am. Chem. Soc.* **1978**, *100*, 5371; b) S. J. Lee, W. Lin, *J. Am. Chem. Soc.* **2002**, *124*, 4554; c) G. A. Hembury, V. V. Borovkov, Y. Inoue, *Chem. Rev.* **2008**, *108*, 1; d) Y. Nishioka, T. Yamaguchi, M. Kawano, M. Fujita, *J. Am. Chem. Soc.* **2008**, *130*, 8160; e) C. Siering, J. Toräng, H. Kruse, S. Grimme, S. R. Waldvogel, *Chem. Commun.* **2010**, *46*, 1625; f) C. Zhao, Q.-F. Sun, W. M. Hart-Cooper, A. G. DiPasquale, F. D. Toste, R. G. Bergman, K. N. Raymond, *J. Am. Chem. Soc.* **2013**, *135*, 18802; g) C. Gütz et al., *Angew. Chem. Int. Ed.* **2014**, *53*, 1693; *Angew. Chem.* **2014**, *126*, 1719.
[7] H. Jędrzejewska, A. Szumna, *Chem. Rev.* **2017**, *117*, 4863.
[8] a) M. A. Masood, E. J. Enemark, T. D. P. Stack, *Angew. Chem. Int. Ed.* **1998**, *37*, 928; *Angew. Chem.* **1998**, *110*, 973; b) A. Lützen, M. Hapke, J. Griep-Raming, D. Haase, W. Saak, *Angew. Chem. Int. Ed.* **2002**, *41*, 2086; *Angew. Chem.* **2002**, *114*, 2190; c) U. Kiehne, T. Weilandt, A. Lützen, *Org. Lett.* **2007**, *9*, 1283; d) C. Maeda, T. Kamada, N. Aratani, A. Osuka, *Coord. Chem. Rev.* **2007**, *251*, 2743; e) G. Meyer-Eppler, F. Topić, G. Schnakenburg, K. Rissanen, A. Lützen, *Eur. J. Inorg. Chem.* **2014**, 2495; f) S. A. Boer, D. R. Turner, *Chem. Commun.* **2015**, *51*, 17375; g) L.-L. Yan, C.-H. Tan, G.-L. Zhang, L.-P. Zhou, J.-C. Bünzli, Q.-F. Sun, *J. Am. Chem. Soc.* **2015**, *137*, 8550; h) V. E. Pritchard, D. Rota Martir, S. Oldknow, S. Kai, S. Hiraoka, N. J. Cookson, E. Zysman-Colman, M. J. Hardie, *Chem. Eur. J.* **2017**, *23*, 6290; i) T. Tateishi, T. Kojima, S. Hiraoka, *Commun. Chem.* **2018**, *1*, 727.
[9] L.-L. Yan, C.-H. Tan, G.-L. Zhang, L.-P. Zhou, J.-C. Bünzli, Q.-F. Sun, *J. Am. Chem. Soc.* **2015**, *137*, 8550.
[10] D. Beaudoin, F. Rominger, M. Mastalerz, *Angew. Chem. Int. Ed.* **2017**, *56*, 1244; *Angew. Chem.* **2017**, *129*, 1264.
[11] a) T. W. Kim, J.-I. Hong, M. S. Lah, *Chem. Commun.* **2001**, 743; b) C. G. Claessens, T. Torres, *J. Am. Chem. Soc.* **2002**, *124*, 14522; c) T. Weilandt, U. Kiehne, G. Schnakenburg, A. Lützen, *Chem. Commun.* **2009**, 2320; d) C. S. Arribas, O. F. Wendt, A. P. Sundin, C.-J. Carling, R. Wang, R. P. Lemieux, K. Wärnmark, *Chem. Commun.* **2010**, *46*, 4381.
[12] a) D. Rota Martir, D. Escudero, D. Jacquemin, D. B. Cordes, A. M. Z. Slawin, H. A. Fruchtl, S. L. Warriner, E. Zysman-Colman, *Chem. Eur. J.* **2017**, *23*, 14358; b) X.-Z. Li, L.-P. Zhou, L.-L. Yan, D.-Q. Yuan, C.-S. Lin, Q.-F. Sun, *J. Am. Chem. Soc.* **2017**, *139*, 8237.
[13] M. Frank, M. D. Johnstone, G. H. Clever, *Chem. Eur. J.* **2016**, *22*, 14104.
[14] A. Westcott, J. Fisher, L. P. Harding, P. Rizkallah, M. J. Hardie, *J. Am. Chem. Soc.* **2008**, *130*, 2950.
[15] R. Weitzenböck, H. Lieb, *Monatsh. Chem.* **1912**, *33*, 549.
[16] a) M. Gingras, *Chem. Soc. Rev.* **2013**, *42*, 968; b) N. Saleh, C. Shen, J. Crassous, *Chem. Sci.* **2014**, *5*, 3680; c) C.-F. Chen, Y. Shen, *Helicene Chemistry*, Springer, Berlin, Heidelberg, **2017**; d) K. Mori, T. Murase, M. Fujita, *Angew. Chem. Int. Ed.* **2015**, *54*, 6847; *Angew. Chem.* **2015**, *127*, 6951; e) J. R. Brandt, X. Wang, Y. Yang, A. J. Campbell, M. J. Fuchter, *J. Am. Chem. Soc.* **2016**, *138*, 9743.
[17] a) T. Verbiest, S. Van Elshocht, M. Kauranen, L. Hellemans, J. Snauwaert, C. Nuckolls, T. J. Katz, A. Persoons, *Science* **1998**, *282*, 913; b) T. Kaseyama, S. Furumi, X. Zhang, K. Tanaka, M. Takeuchi, *Angew. Chem. Int. Ed.* **2011**, *50*, 3684; *Angew. Chem.* **2011**, *123*, 3768.
[18] a) A. Terfort, H. Görls, H. Brunner, *Synthesis* **1997**, 79; b) J. M. Fox, D. Lin, Y. Itagaki, T. Fujita, *J. Org. Chem.* **1998**, *63*, 2031.
[19] a) S. Löffler, J. Lübben, A. Wuttke, R. A. Mata, M. John, B. Dittrich, G. H. Clever, *Chem. Sci.* **2016**, *7*, 4676; b) S. Freye, R. Michel, D. Stalke, M. Pawliczek, H. Frauendorf, G. H. Clever, *J. Am. Chem. Soc.* **2013**, *135*, 8476.
[20] S. Parsons, H. D. Flack, T. Wagner, *Acta Crystallogr. Sect. B* **2013**, *69*, 249.
[21] G. M. Sheldrick, *Acta Crystallogr. Sect. C* **2015**, *71*, 3.
[22] Y. Nakai, T. Mori, Y. Inoue, *J. Phys. Chem. A* **2012**, *116*, 7372.
[23] Y. Nakai, T. Mori, Y. Inoue, *J. Phys. Chem. A* **2013**, *117*, 83.
[24] G. M. Sheldrick, *Acta Crystallogr. Sect. A* **2015**, *71*, 3.
[25] P. Thordarson, *Chem. Soc. Rev.* **2011**, *40*, 1305.
[26] a) O. Jurček, P. Bonakdarzadeh, E. Kalenius, J. M. Linnanto, M. Groessl, R. Knochenmuss, J. A. Ihalainen, K. Rissanen, *Angew. Chem. Int. Ed.* **2015**, *54*, 15462; *Angew. Chem.* **2015**, *127*, 15682; b) J.-F. Greisch, J. Chmela, M. E. Harding, D. Wunderlich, B. Schäfer, M. Ruben, W. Klopper, D. Schooss, M. M. Kappes, *Phys. Chem. Chem. Phys.* **2017**, *19*, 6105.
[27] G. H. Clever, S. Tashiro, M. Shionoya, *J. Am. Chem. Soc.* **2010**, *132*, 9973.
[28] a) A. U. Malik, F. Gan, C. Shen, N. Yu, R. Wang, J. Crassous, M. Shu, H. Qiu, *J. Am. Chem. Soc.* **2018**, *140*, 2769; b) T. Matsushima, S. Kikkawa, I. Azumaya, S. Watanabe, *ChemistryOpen* **2018**, *7*, 278.
[29] A. Burkhardt, T. Pakendorf, B. Reime, J. Meyer, P. Fischer, N. Stübe, S. Panneerselvam, O. Lorbeer, K. Stachnik, M. Warmer, P. Rödig, D. Göries, A. Meents, *Eur. Phys. J. Plus* **2016**, *131*, 56.

Manuscript received: November 11, 2018
Revised manuscript received: February 10, 2019
Accepted manuscript online: February 13, 2019
Version of record online: March 21, 2019

